AR-010-256

DSTO-TR-0549

Stress Analysis of an Interference Fit Life Extension Option for a Cold Expanded Elongated Fuel Flow Vent Hole on the F-111C Aircraft

R.B. Allan and M. Heller

DSTO-TR-0549

DEPARTMENT OF DEFENCE
DEFENCE SCIENCE AND TECHNOLOGY ORGANISATION

Stress Analysis of an Interference Fit Life Extension Option for a Cold Expanded Elongated Fuel Flow Vent Hole on the F-111C Aircraft

R. B. Allan & M. Heller

Airframes and Engines Division
Aeronautical and Maritime Research Laboratory

DSTO-TR-0549

ABSTRACT

This investigation has been undertaken as part of a program of work having the aim of determining a suitable fatigue life enhancement option for the non-circular fuel flow vent hole number 13 in the wing pivot fitting of the F-111C aircraft. Two types of stress analysis have been undertaken for a finite width rectangular plate of D6ac steel containing an elongated hole. Firstly, plate stress distributions due to interference fitting obtained from elastic two dimensional finite element analyses were compared to those measured experimentally using strain gauges and thermoelasticity. Secondly, two-dimensional elastic-plastic finite element analyses were undertaken to quantify the effect on critical plate stresses due to enhancement by combined cold expansion with interference fitting, in the presence of subsequent representative cold proof test loading and a sample spectrum loading. The predicted stresses for the elastic analysis cases agreed well with the experimental results, which also demonstrated the suitability of a proposed tapered plug/sleeve design to achieve effective interference fitting of an elongated hole. Overall, enhancement through combined cold expansion and interference fitting was considered to be significantly better than interference fitting alone. For example, the combined enhancement case, as compared to interference fitting only, led to a change in the critical hoop stress from 603 MPa, to -87 MPa. These favourable results indicate that such an enhancement procedure would potentially be suitable for extending the fatigue life of the fuel flow vent hole number 13 region of the F-111C aircraft, pending the results of appropriate static and fatigue tests.

RELEASE LIMITATION

Approved for public release

DEPARTMENT OF DEFENCE

DEFENCE SCIENCE AND TECHNOLOGY ORGANISATION

Published by

DSTO Aeronautical and Maritime Research Laboratory
PO Box 4331
Melbourne Victoria 3001

Telephone: (03) 9626 7000
Fax: (03) 9626 7999

AR-010-256
June 1997

APPROVED FOR PUBLIC RELEASE

Stress Analysis of an Interference Fit Life Extension Option for a Cold Expanded Elongated Fuel Flow Vent Hole on the F-111C Aircraft

Executive Summary

An area of major concern for the F-111C airframe in service with the RAAF is the wing pivot fitting in which there are a number of non-circular (elongated) machined fuel flow vent holes. There have been numerous incidents of fatigue cracks at fuel flow vent hole number 13, and the problem could compromise the structural integrity of the F-111C fleet out to the planned withdrawal date of 2020. Currently, the problem is being managed by reshaping periodically the fuel flow vent holes to one of a family of progressively larger shapes, thereby removing any existing cracks. Unfortunately, this process does not completely eliminate further cracking, and at the current rate of crack growth and hole reshaping, this method may not enable the aircraft to reach its desired service life.

The present investigation has been undertaken as part of a program of work having the aim of determining a suitable fatigue life enhancement option for the non-circular fuel flow vent hole number 13 in the wing pivot fitting of the F-111C aircraft. Two types of stress analysis have been undertaken for a finite width rectangular plate of D6ac steel containing an elongated hole. Firstly, plate stress distributions due to interference fitting obtained from elastic two dimensional finite element analysis were compared to those measured experimentally using strain gauges and thermoelasticity. Secondly, two-dimensional elastic-plastic finite element analyses were undertaken to quantify the effect on critical plate stresses due to enhancement by combined cold expansion with interference fitting, in the presence of subsequent representative cold proof test loading (CPLT) and a sample spectrum loading. The predicted stresses for the elastic analysis cases agreed well with the experimental results, which also demonstrated the suitability of a proposed tapered plug/sleeve design to achieve effective interference fitting of an elongated hole. Overall, enhancement through combined cold expansion and interference fitting was considered to be significantly better than interference fitting alone.

These favourable results indicate that such an enhancement procedure would potentially be suitable for extending the fatigue life of the fuel flow vent hole number 13 region of the F-111C aircraft, pending the results of appropriate static and fatigue tests.

Authors

R.B. Allan
Airframes and Engines Division

Robert Allan completed a B. Eng. (Aeronautical) at R.M.I.T. in 1978. Since then he has worked in the areas of aircraft structural design, repair and manufacturing at major Australian and U.S. aircraft companies. Some major projects worked on in this time were the tailplane and elevator design of the Wamira aircraft project, F/A-18 aft fuselage redesign and the support of local manufacture of numerous aircraft components. Prior to joining AMRL in 1994, he spent 5 years in the field of polymer flow characterisation and simulation using finite element methods, gaining a broad knowledge of finite element stress analysis. Since joining AMRL he has worked in the area of life extension through the use of structural mechanics in support of Australian Defence Force aircraft, specialising in finite element stress analysis and advanced experimental stress analysis.

M. Heller
Airframes and Engines Division

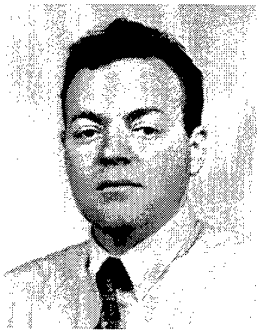

Manfred Heller completed a B. Eng. (Hons.) in Aeronautical Engineering at the University of New South Wales in 1981. He was awarded a Department of Defence Postgraduate Cadetship in 1986, completing a PhD at Melbourne University in 1989.

He commenced work in Structures Division at the Aeronautical Research Laboratory in 1982. He has an extensive publication record focussing on the areas of stress analysis, fracture mechanics, fatigue life extension methodologies and experimental validation. Since 1992 he has led tasks which develop and evaluate techniques for extending the fatigue life of ADF aircraft components and provide specialised structural mechanics support to the ADF. He is currently a Senior Research Scientist in the Airframes and Engines Division.

Contents

Notation

σ	stress
ν	Poisson's Ratio
δ	radial interference ($\delta=r_m-a$)
E	elastic modulus
GPa	giga pascals
mm	millimetres
MPa	mega pascals
r	radius
u	radial displacement of node on mandrel/hole boundary
v	hoop displacement of node on mandrel/hole boundary
x, y	Cartesian co-ordinates

Subscripts

θ	hoop
m	mandrel (also plug)
p	plate
r	radial
0	yield

List of Abbreviations

AMRL	Aeronautical and Maritime Research Laboratory
CPLT	cold proof load test (The F-111C airframe is subjected to this static proof loading periodically to determine its damage tolerance)
DADTA	durability and damage tolerance analysis
FAST	Focal-plane Array for Synchronous Thermography
FFVH	fuel flow vent hole
FFVH13	fuel flow vent hole number 13
RAAF	Royal Australian Air Force
SPATE	Stress Pattern Analysis by measurement of Thermal Emission

1. Introduction

An area of major concern in the F-111C airframe is the wing pivot fitting manufactured from D6ac steel. It contains a number of machined fuel flow vent holes (FFVH), as shown in Figure 1. Under cold proof load tests (CPLT), the material around hole #13 (i.e. FFVH13), experiences extensive plastic deformation, which results in the introduction of residual stresses. These residual stresses coupled with the local material response due to the remote loading sequence experienced in service are detrimental, and contribute to crack initiation and growth in this region. There have been numerous incidents of fatigue cracking at FFVH13 in the wing pivot fitting in the F-111C fleet, and the problem could compromise the structural integrity of these aircraft out to the planned withdrawal date of 2020.

Currently, the problem is being managed by reshaping FFVH13 to one of a family of progressively larger shapes [1], and thereby removing any existing cracks. The extent of the rework depends on the size of the detected crack. For example Figure 2 shows the original geometry for FFVH13 as well as two typical rework shapes. Unfortunately, the reworking procedure does not completely eliminate further cracking, and at the current rate of crack growth and the reworking frequency, this method may not be sufficient to enable the aircraft to reach its desired service life. A durability and damage tolerance analysis (DADTA) is presently being used to certify the use of these rework shapes as a valid means for managing this critical location. If the reworking procedure cannot allow the aircraft to reach the desired service life, an alternative method of life extension will be required. In view of this problem, AMRL has been tasked with the development of a proposed non-circular cold expansion/interference fit plug option, for the life extension of FFVH13, with the aim of eliminating crack growth or significantly reducing the crack growth rate.

The typical benefit of cold expansion and/or interference fitting for the life extension of plates containing circular holes is reasonably well established and documented. For example, the use these procedures has been reviewed by Mann and Jost [2]. Closed form theoretical solutions only apply to the simplest configurations, so typically finite element analyses are employed to solve problems of practical importance. However, previous work in the literature does not give clear guidelines for either: (i) non-circular geometries, or (ii) complex remote loading conditions and realistic strain hardening material properties. Both of these issues need to be addressed when developing a life extension option for the FFVH13 on the F-111C aircraft. Recent work by the authors [3] has however addressed the second issue for an enhanced circular hole to gain a preliminary understanding of the interaction of the key parameters involved.

In this report both pertinent issues are addressed, where the key geometric, material and loading parameters have been chosen to be representative of the FFVH13 region of the F-111C aircraft. In Section 2 the process definitions for cold expansion and interference fitting are provided, and their effect on stress values at the hole edge is

explained generically. The finite element and experimental methods used in the investigation are presented in Sections 3 and 4 respectively. In Sections 5 to 7 the results of two types of stress analysis are given for a finite width rectangular plate of D6ac material containing an enhanced elongated hole. Firstly, plate stress distributions due to interference fitting obtained from elastic two dimensional finite element analysis are compared to those measured experimentally using strain gauges and thermoelasticity. Secondly, results from two-dimensional elastic-plastic finite element analyses are given to quantify the effect on critical plate stresses due to enhancement by interference fitting with or without prior cold expansion, in the presence of a subsequent representative CPLT and a sample spectrum loading. A convenient summary of key finite element results is then given in Section 8 followed by conclusions in Section 9.

2. Background to Cold Expansion and Interference Fitting Processes

2.1 Process Definitions

It is considered helpful to highlight the key similarities and differences between these two enhancement procedures. Unfortunately no work in the open literature discusses either of this processes in the context of non-circular (i.e. elongated) holes. However, as a first estimate it is reasonable to expect that the effect of these enhancement processes will be similar for both circular and elongated holes. Hence for the case of a plate containing an enhanced circular hole the key features of cold expansion and interference fitting, (see also Broek [4] and Jost [5] & [6]) can be explained as follows.

In the ***Cold expansion*** process, the hole is initially expanded to a level sufficient to cause local yielding to occur. This is typically achieved by passage of an oversize tapered mandrel (such as a plug) or a mandrel/sleeve combination through the hole. Then the mandrel is removed from the hole, and the surrounding elastically deformed material forces a reduction in hole diameter from the fully expanded size. This results in a zone around the hole containing residual compressive hoop stresses. As the extent of yielding during expansion is increased, the larger is the zone of induced compressive stress. Depending on the degree of expansion, compressive reyielding on mandrel removal can also occur, although the size of this reyielded zone is substantially less than that generated by the mandrel enlarging the hole. Under the influence of cyclic remote loading, the presence of the compressive zone at the hole boundary causes the mean of the induced local cyclic stresses to be significantly less than for a non-cold expanded hole. Although the magnitude of the local cyclic stress range is typically unchanged as compared to the non cold expanded hole, the tensile part of the cycle is substantially reduced. Hence the reduction in mean local stress at the hole boundary is typically highly beneficial in delaying the onset of crack initiation and hence increasing fatigue life of a component with a cold expanded hole.

Interference fitting is the process of installing an oversized mandrel (such as a plug) into the hole. This is often achieved by passage of a tapered mandrel into the hole until a required interference level is obtained. Unlike the cold expansion process, the mandrel remains *in situ* and typically plate deformation due to the interference fitting process is elastic. This process has two effects. Firstly, a residual tensile circumferential stress is induced in the plate at the hole boundary. Secondly, the *in situ* mandrel provides an alternative load path when the plate is subjected to remote cyclic loading, thereby reducing the magnitude of local cyclic stresses in the plate at the hole boundary. Typically, the reduction in the magnitude of the local cyclic stresses is highly beneficial in delaying the onset of crack initiation and hence increasing fatigue life. However caution must be exercised when assessing the potential benefit of this approach, particularly if the remote loading sequence is dominated by compressive loads. In such a case (even though the magnitude of local cyclic stress at the hole edge is reduced), the higher mean stress due interference fitting signifies that the application of both tensile and compressive loading will cause local fatigue damage accumulation. From the above, the potential improvement in fatigue life of a component with an interference fitted hole will depending on the particular remote loading sequence, and on the magnitude of the mean stress due to interference fitting.

2.2 Combined Effects

Based on the description given in Section 2.1, it is expected that greatest benefit to fatigue life extension will result from a combination of hole cold expansion followed by interference fitting. In prior work [3], a detailed plane-strain, elastic-plastic finite element analysis of such a situation for a D6ac plate containing an enhanced ***circular*** hole was undertaken. Here F-111C representative loading was applied to the plate as follows: (i) a CPLT sequence of 0, 228, -556, 228, -556, and 0 MPa, followed by (ii) a sample spectrum loading of ±200 MPa. This analysis addressed the following pertinent enhancement cases assuming a strain hardening material constitutive response: (i) unenhanced open circular hole, (ii) 0.5% interference fitted plug (D6ac material) only, and (iii) combined 1.5% cold expansion and 0.5% interference fitting. The stress histories at the critical location on hole edge for these three cases are presented in Figure 3. To aid comparison the mean and cyclic stress responses during the sample spectrum loading (i.e. after enhancement and CPLT) are given in Table 1. The following key findings are apparent:

(i) For the unenhanced open hole, application of the CPLT results in a significant residual tensile hoop stress of 200 MPa, at the critical location on the hole edge. Hence during application of the remote loading, the mean stress was 200 MPa and the cyclic stress concentration factor was 3.1.

(ii) For both enhancement cases, the stress response during the sample remote loading subsequent to the CPLT was linear, with a cyclic stress concentration factor of unity.

(iii) Enhancement through combined cold expansion and interference fitting was significantly better than interference fitting alone. For the enhanced case with cold expansion of 1.5% followed by interference fitting of 0.5%, there was a residual (compressive) hoop stress of -1080 MPa as compared to a residual (tensile) hoop stress of 350 MPa for the interference fitting only case.

(iv) Overall, enhancement through combined cold expansion with interference fitting is considered highly beneficial, with the favourable stresses generated not adversely affected by subsequent CPLT.

Table 1: Hoop stresses at the critical location in an enhanced plate containing a circular hole due to a sample remote loading of ±200 MPa after CPLT (Figure 3).

Enhancement case	Mean hoop stress (MPa)	Cyclic hoop stresses (MPa)	Stress concentration
Open hole	200	-415 to 817	3.1
1.5 % cold expansion with 0.5% interference fit	-1080	-1280 to -880	1.0
0.5% interference fit	551	350 to 751	1.0

Hence, in the context of the present work, it is reasonable to expect that the benefit indicated by the combined enhancement approach for an elongated hole will be similar to that demonstrated in the prior work on the circular hole case.

3. Finite Element Method

In this work, elastic and plastic plane strain analyses have been undertaken using the PAFEC finite element code, level 8 running on a Hewlett Packard K series 9000 computer at AMRL. Eight-noded isoparametric quadrilateral elements were used for all analyses. The plasticity subroutines in PAFEC make use of the Prandtl-Reuss equations in conjunction with the von Mises yield criterion and an isotropic hardening model. For all plastic analyses loads were applied incrementally, with further iterations undertaken for each increment until acceptable convergence to the material non-linear stress-strain constitutive response curve was achieved. The convergence criteria were judged to be achieved when the internal energy was less than 1% different to the external work due to the applied loads, for a given increment. For a typical plastic analysis, the following number of non-uniform increments were used: (i) twelve displacement increments for the cold expansion process, (ii) ten displacement increments for subsequent interference fitting, (iii) thirty five load increments for the CPLT, and (iv) fourteen load increments for the sample remote spectrum loading.

3.1 Geometry and Loading

The geometry relevant to the two dimensional idealisation of the enhanced elongated hole in a remotely loaded rectangular plate specimen is shown in Figure 4(a). The plate is 76 mm wide, 245 mm long and has a thickness of 5 mm. The hole in the plate is 50.8 mm long and 25.4 mm wide and its major axis is oriented at an angle of 16 degrees relative to the remote loading axis. The size of the elongated hole has been chosen to be similar to the maximum AMRL rework size as shown in Figure 2, hence it could be applied to most holes in the fleet, irrespective of their current hole shape (due to prior reworking). The hole orientation of 16 degrees was chosen to locate the maximum hoop stress at the hole edge, in the same position as determined for an actual representative geometry and loading of the FFVH13 in the wing pivot fitting, [1]. This feature is well demonstrated by inspection of the contours of von Mises stress obtained from elastic finite element analysis shown in Figure 5. This figure refers to the following cases: (i) the figure on the left gives the peak stress at point A for an analysis of a representative wing substructural model which includes the skin, and (ii) the figure to the right gives the peak stress at point B for an analysis of the plate specimen (unenhanced). It can be seen that points A and B on the respective models are at the same location with respect to the hole. The overall finite element mesh used to model the plate is shown in Figures 6, while a more detailed view showing the region near the hole is given in Figure 7.

The idealised two dimensional interference fit plug geometry is shown in Figure 4(b) for the case of 0.5 % interference. Here the plug is 51.05 mm long, 25.525 mm wide and 5 mm thick. For all analyses the length of the flat sides is kept constant, while different levels of interference are modelled as described in Section 3.2. The hole in the middle of the plug represents a bolt hole which is required to install the plug (Section 4). It should be noted that the plug (insert) geometry used in the experiments has some differences to this two dimensional finite element idealisation as follows: (i) the actual plug (insert) is slightly tapered in the out of plane direction, (ii) the actual plug contains two holes instead of one, and (iii) the actual plug consists of two components (plug and sleeve). As this report presents only the stresses in the plate it is considered that the idealisation is appropriate. The overall finite element mesh used to model the plate with the plug inserted is shown in Figure 8, while a more detailed view showing the region around the plug hole is given in Figure 9. The finite element model representing the plate with the plug consisted of approximately 1921 isoparametric rectangular and triangular elements.

For all analyses the remote loading to the coupon was applied after enhancement, and one of two analysis types was undertaken; with either elastic or elastic-plastic material constitutive properties. In the case of the elastic analyses, a suitable value of the remote loading was chosen to enable comparison to the results of the experimental work. In the case of the elastic plastic analyses, the plate was subjected to F-111C representative loading conditions. Here the representative loading consisted of: (i) a CPLT sequence of 0, 228, -556, 228, -556, and 0 MPa, followed by (ii) a sample spectrum loading of ±200 MPa.

3.2 Interference and Cold Expansion Modelling

3.2.1 Elastic Interference Cases

The formulation of the required interference constraint conditions in the finite element model can be described by considering two typical adjacent points (A and B) at the interface of the mandrel (or plug) and the plate (at the hole edge), as shown prior to mandrel insertion in Figure 10. After insertion these two points become coincident for the no slip (i.e. no relative displacement in the tangential direction) case. Hence the constraint equations in terms of Cartesian displacements per pair of nodes for this case are given in Equations (1) and (2). These equations are then used for all pairs of nodes around the interface. In the case of slip allowed, only the constraint condition given in equation (1) is used. This enables relative displacement in the hoop direction to occur between corresponding nodes at the mandrel and plate interface.

$$u_p - u_m = \delta \tag{1}$$

$$v_p - v_m = 0 \tag{2}$$

3.2.2 Plastic Cases

The plastic analyses for cold expansion and interference fitting were undertaken in a similar manner to the elastic analyses except that the expansion constraint conditions and remote loading were applied in small increments. The only difficulty that arises in using this method is specifying correctly the increment that corresponds to mandrel removal (ie cold expansion removal) for geometries other than the annulus. For the plate geometries which are non-axi-symmetric the hole would end up non-circular after cold expansion. During the iterative finite element analysis, the increment in the cold expansion cycle considered "mandrel removal" was taken to be when the radial stress at the critical location (θ=20°) becomes zero. The relatively small error arising from this assumption, is shown in Figure 11 for the typical case of a cold expanded hole (Section 7), as a function of angular position around the hole boundary as defined in Figure 12. Apart from the peak near θ=0, the error at all other points around the boundary is less than 50 MPa. For comparison purposes, the corresponding residual hoop, maximum radial and maximum hoop boundary stress distributions are also shown in this figure.

3.2.3 General Comments

The analysis procedure presented above is considered valid for the assumed constraint conditions, with the further requirement that no separation at the mandrel/plate interface occurs during remote loading of the plate. In practice these requirements will depend on interference level, the relative material stiffness values of the mandrel and plate, the coefficient of friction at the mandrel/hole interface, and the magnitude of the remote loading.

3.3 Material Properties

Analyses undertaken for the D6ac steel plate specimen and plug used either elastic or elastic-plastic material constitutive response properties, as appropriate. For the elastic analyses the material properties were taken as $E = 207$ GPa and $\nu = 0.33$. For the elastic-plastic analyses the assumed stress-strain response as shown in Figure 13 was used. Here as before the pre-yield material properties were $E = 207$ GPa and $\nu = 0.33$. The non-linear part of the response was well approximated by a piecewise linear representation consisting of 26 segments, with the initial yield point being $\sigma_0 = 1142$ MPa.

4. Experimental Methods

In the experimental program undertaken, two enhancement cases for the plate shown in Figure 4(a) were considered, namely the open hole (i.e. unenhanced) case, and enhancement through interference fitting. The level of plug interference fitting was 0.74%, and hence the induced plate stresses were in the linear elastic regime. Furthermore in both cases the plate remote loading was chosen such that the stress response in the plate was elastic. The experimental program had two aims; firstly to demonstrate the practical viability of the non-circular interference-fit plug design, and secondly to enable comparison of measured strains with the predictions from two dimensional finite element analyses. All testing was conducted using an MTS 320 kN servo hydraulic universal testing machine unless otherwise noted.

4.1 Interference Fitting for Elongated Hole

The arrangement of a plug/sleeve design which was used to achieve interference fitting of the elongated hole is shown schematically in Figure 14. A photograph of the key components is also given in Figure 15, and the relevant engineering drawings are given in Figure 16. The repair concept involves initially placing a neat fitting sleeve into an accurately machined elongated hole. The sleeve has a 1:50 taper on its internal surface that mates with a plug having the same taper on its outer surface. The plug is pulled into the sleeve by tightening two bolts. The sleeve has a split mid-way along one of its flat sides so that expansion is not unduly restricted during the insertion process. Once the interference fit plug has been inserted to a required depth, shims are placed between the backing plate and the plug, and the assembly re-tightened, to ensure that the plug does not work loose under the action of fatigue loading of the plate. The overall design offers a number of useful features including: (i) ease of removal for inspection of the hole when required, (ii) the expansion level can be varied depending on the plug insertion depth, and (iii) the relative material properties of the sleeve and plug can be varied as required. Filling the FFVH13 with an interference fit repair will stop fuel flow, but this is of no consequence since there are many other non-critical fuel flow holes in the wing pivot fitting.

4.2 Stress and Strain Measurements

For all specimens tested, strains were measured using eight uniaxial strain gauges (type TML[1] NFA-1) with their centres located around the hole boundary as shown in Figure 17. Thermolelastic stress measurements were also recorded using either the SPATE 8000 System or the FAST System. These systems were used to give full-field bulk stress measurements for the face of the plate over a scan region encompassing the hole. It is important to note that only cyclic stresses can be measured using these systems, i.e. interference stresses cannot be determined. For tests involving the SPATE 8000 thermoelastic system the remote plate loads were applied sinusoidally at a frequency of 10 Hz. After mounting the specimen in the machine the scan surface was cleaned and sprayed with matt black paint to enhance response. The applied cyclic load amplitude was ±20 kN with a mean of 20.5 kN. The SPATE detector head was placed 580 mm from the specimen surface at an angle of 30 degrees. The scan size was 212 x 248 sample points and the scan time took approximately 4.5 hours. For tests involving the FAST thermoelastic system the specimen was mounted in a MTS 50 kN axial test machine and loads were applied sinusoidally at a frequency of 4 Hz. The applied cyclic load amplitude was ±10 kN with a mean of 15 kN. The FAST scans typically took 20 minutes. After recording, all theromelastic measurements were calibrated using a linear scaling factor, to allow comparison with the finite element results.

5. Plate with Unenhanced Elongated Hole

For the plate with the unenhanced hole two types of analyses were considered. Firstly elastic analyses were undertaken where the remote uniaxial load was of arbitrary magnitude to enable comparison of elastic stress distributions determined from two dimensional finite element analysis to those measure experimentally. Secondly elastic plastic finite element analyses were undertaken where representative F-111C loading was applied to the plate as follows: (i) a CPLT sequence of 0, 228, -556, 228, -556, and 0 MPa, followed by (ii) a sample spectrum loading of ±200 MPa.

5.1 Elastic Analysis

Strain gauge results (specimen EM47AG1A) are given in Table 2 where they are compared with the predictions from finite element analysis. It can be seen that relatively good correlation was achieved. In particular, at the location of highest hoop stress (gauge 1), the finite element prediction is within 5% of the measured value.

[1] TML is a trademark of Tokyo Sokki Kenkyujo Co. Ltd, Japan.

Table 2: Comparison of strain gauge and finite element results for plate specimen with an unenhanced elongated hole for a remote loading of 100 MPa.

Gauge Number	Strain gauge (με)	FE Strain (με)
1	1124	1180
2	-129	-185
3	241	411
4	603	674
5	-176	-315
6	-179	-325
7	1289	1059

The cyclic bulk stress distribution, determined from the finite element analysis is shown in Figure 18, for a remote loading range of 0 to 100 MPa. The corresponding calibrated experimental measurements obtained using the SPATE and FAST systems, are given in Figures 19 and 20 respectively The experimentally determined plate bulk stresses peaked at approximately 490 MPa, as compared to 562 MPa from the finite element analysis. This slight difference is as expected since at the free edge of a stress concentrator thermoelastic measurements always underestimate the magnitude of the stress peak, (due to the finite size of each pixel, some part of which will in general be off the free edge of the specimen).

5.2 Elastic-Plastic Finite Element Analysis

The hoop stress results at the critical location, (point A, Figure 12) on the hole edge are given in Figure 21. It can be seen that the stress response is elastic during the application and removal of the remote tensile loading of 228 MPa. However the high remote compressive loading to -556 MPa causes material yielding, and upon its removal , a residual tensile hoop stress of 773 MPa is induced. Subsequently, due to the application and removal of the remote loading of 228 MPa, (which causes tensile yielding), the residual stress becomes 552 MPa. The final part of the CPLT, a compressive loading to -556 MPa causes material yielding to again occur in compression, such that upon its removal the residual tensile hoop stress is 685 MPa. The stress response due to the sample remote loading is linear, and hence a residual hoop stress of 685 MPa exists at the end of this loading sequence. Since the hole is unfilled, the cyclic stress concentration due to this loading is 4.1.

6. Plate with Elongated Hole Enhanced by an Interference Fit Plug

Here two types of analyses were considered. Firstly elastic analyses were undertaken where the remote uniaxial load was of arbitrary magnitude to enable comparison of elastic stress distributions determined from two dimensional finite element analysis to those measured experimentally. Secondly elastic plastic finite element analyses were undertaken where representative F-111C loading was applied to the plate as follows: (i) a CPLT sequence of 0, 228, -556, 228, -556, 0 MPa, followed by (ii) a sample spectrum loading of ±200 MPa.

6.1 Elastic Analysis

The results for the radial and hoop stresses around the hole boundary, due to 0.74% interference fitting, are given in Figure 22. It should be noted here that the co-ordinate system here is different to that used in Figure 12. Figure 22 shows a number of important features as follows: (i) unlike a circular hole case, the stress distribution is non-uniform, (ii) there is a very steep change in hoop stress in the region of θ=45° and θ=135°, changing from compressive to tensile, and (iii) tensile hoop stresses are only induced in the curved section. The corresponding full field bulk stress distribution for the coupon due to interference fitting is shown in Figure 23, and highlights the non-uniform nature of the in plane stresses. Strain gauge results after interference fitting (specimen EM47AS1A) are given in Table 3, where they are compared with the predictions from finite element analysis. It is evident that the important peak tensile and compressive stresses are well predicted at gauges 2 and 6. As can be expected the agreement at the tangent point (θ=45°), ie gauges 1,3 and 7, was poorer, due to the very high stress gradient at that location (Figure 22).

Table 3: Comparison of strain gauge and elastic finite element results for plate specimen due to 0.74%[2] interference fit plug in an elongated hole (no remote loading).

Gauge number	Strain gauge results(με)	Finite element results(με)
1	755	1494
2	3721	4157
3	1563	1638
4	277	-155
5	-850	-722
6	-1065	-815
7	1319	2198

[2] The interference level was determined after the test data had been plotted, and a corrected zero level had been found.

The cyclic bulk stress distribution, determined from the finite element analysis is shown in Figure 24, for a remote loading range of 0 to 100 MPa. The corresponding calibrated experimental measurements obtained using the SPATE system is given in Figure 25. Both figures confirm that the cyclic stress distribution has been rendered much more uniform due to the interference fit plug as compared to the open hole case (figures 19 and 20). The stress concentration factor has been reduced from 4.5 for the open hole to 1.5 for the plugged hole. The experimentally determined plate bulk stresses peaked at approximately 159 MPa, as compared to 150 MPa from the finite element analysis. However it should be noted that the location of the two peaks is different. This can be attributed to the fact that the finite element analysis is based on an idealised two dimensional geometry, whereas the experimental arrangement is a complex three dimensional geometry, where the material thickness of the plug assembly is significantly greater than the plate thickness. Hence the out of plane three dimensional load paths in the plugged region are unknown.

In Table 4 a comparison of strain gauge and finite element results due to remote cyclic loading for the plugged elongated coupon is given. The strain gauge results are in reasonable agreement with the finite element predictions, and are consistent with the results of the SPATE analysis.

Table 4: Comparison of cyclic strain gauge and elastic finite element results for plate specimen containing a interference fit plug due to a remote loading range of 0 to 100 MPa.

Gauge number	Strain gauge results(με)	Finite element results(με)
1	303	457
2	-206	-109
3	289	435
4	396	408
5	-65	-77
6	-17	-325
7	262	446

6.2 Elastic-Plastic Finite Element Analyses

The interference level here was chosen to be 0.5% to be consistent with prior work on a plate containing an enhanced circular hole [3]. The analysis results obtained for this enhancement case, assuming no-slip, are shown in Figure 26, at the critical location (Point A). It can be seen that the plate stress response is elastic during the plug insertion and all subsequent remote loading. Clearly as a result of interference fitting the mean stress during the sample remote loading is relatively high at 603 MPa, however the cyclic stress concentration has been reduced to 1.1. The corresponding results for the slip allowed case are presented in Figure 27. This causes two significant changes to the response during remote loading; (i) the mean stress is lower at 364 MPa, and (ii) the cyclic stress concentration is somewhat higher at 1.5. These results are

consistent with the fact that when slip is allowed to occur the amount of load transferred between the plug and plate is reduced.

7. Plate with Elongated Hole Enhanced by Cold Expansion Followed by Interference Fitting

Here elastic-plastic finite element analyses were undertaken where the plate with the enhanced hole was subjected to the following F-111C representative remote loading conditions: (i) a CPLT sequence of 0, 228, -556, 228, -556, and 0 MPa, followed by (ii) a sample spectrum loading of ±200 MPa. Enhancement of the hole consisted of 1.5% cold expansion followed by 0.5% interference fitting. The results obtained for this enhancement case, assuming no-slip, are shown in Figure 28, at the critical location (Point A). It can be seen that the cold expansion process causes a residual compressive hoop stress of -670 MPa. Due to subsequent interference fitting the residual compressive hoop stress is -87 MPa. It is also seen that material yielding does not occur during the subsequent application of the CPLT and sample remote loading. Hence the mean stress during the sample remote loading is compressive at -87 MPa. As expected, the cyclic stress concentration of 1.1 is the same as for the enhancement case consisting of interference fitting only (Section 5.2). It is relevant to note the permanent deformation (deflection) of the hole boundary after the cold expansion process, as shown in Figure 29. In this Figure the deflection distribution is shown for one half of the symmetric elongated hole, where the angular position is as defined in Figure 12. There are two interesting aspects to these results as follows: (i) the average deformation of 0.0344 mm ± 0.0054 mm compares well with analogous results for a circular hole case of 0.0301 mm ± 0.000075 mm [3], and (ii) the deflections along the flat sides of the hole (-45° to 0° and 180° to 225°) are somewhat higher than for the end radius.

8. Summary of Finite Element Results

In the previous Sections 5, 6 and 7, the hoop and radial stress responses have been presented in detail for various enhancement cases. In the context of fatigue life extension, the quantities of key interest are the mean and hoop stress responses due to remote loading at the critical location (point A, Figure 12). To allow for a convenient comparison, the results of elastic analyses for the plate containing either an unenhanced or interference fitted hole are given in Table 5. In this table the analogous results [3] for a large plate containing a circular hole are also given. The key results obtained for the elastic-plastic stress analysis of the plate with the enhanced elongated hole, and subjected to the CPLT are given in Table 6. In the table the analogous results for a large plate containing an circular enhanced hole [3] are also given. Furthermore, hoops stress response histories are plotted in Figure 30, which can be directly compared to those for the circular hole case given earlier in Figure 3.

Table 5: Elastic hoop stresses at the critical location in an enhanced plate containing a circular or elongated hole due to a sample remote loading of ±200 MPa (Figure 3).

Enhancement case	Mean hoop stress (MPa)	Cyclic hoop stresses (MPa)	Stress concentration
Open hole			
- round hole [3]	0	-620 to 620	3.1
- elongated hole	0	-820 to 820	4.1
0.5% interference fit plug			
- round hole [3]	551	-200 to 200	1
- round hole, slip allowed [3]	389	31 to 747	1.79
- elongated hole	604	384 to 824	1.1
- elongated hole, slip allowed	364	-177 to 906	1.5

Table 6: Hoop stresses at the critical location in an enhanced plate containing a circular or elongated hole due to a sample remote loading of ±200 MPa after CPLT (Figure 30).

Enhancement case	Mean hoop stress (MPa)	Cyclic hoop stresses (MPa)	Stress concentration
Open hole			
round hole [3]	200	-415 to 817	3.1
elongated hole	685	-120 to 1506	4.1
0.5% interference fit plug			
round hole [3]	551	350 to 751	1.0
round hole, slip allowed [3]	389	31 to 741	1.79
elongated hole	604	384 to 824	1.1
elongated hole, slip allowed	364	-177 to 906	1.5
1.5% cold expansion and 0.5% interference fit plug			
round hole [3]	-1080	-1280 to -880	1.0
round hole, slip allowed [3]	-1071	-1429 to -720	1.79
elongated hole	-87	-306 to 132	1.1

9. Conclusions

This report presents the detailed stress responses for a finite width rectangular plate of D6ac material containing an enhanced elongated hole, for two distinct analysis cases. Firstly, elastic analyses were undertaken where the remote uniaxial load was of arbitrary magnitude to enable comparison of elastic stress distributions determined from two dimensional finite element analysis to those measured experimentally. Secondly, elastic plastic finite element analyses were undertaken where representative F-111C loading was applied to the plate as follows: (i) a cold proof test loading (CPLT) sequence of 0, 228, -556, 228, -556, and 0 MPa, followed by (ii) a sample spectrum loading of ±200 MPa.

9.1 Elastic Analyses

For this case the present study indicates the following key points:

(i) The finite element analyses have predicted that for an elongated (non-circular) hole, enhancement with an interference fit plug reduces the cyclic stress concentration factor from 4.1 to 1.1 assuming no-slip. The corresponding induced mean stress is 604 MPa.

(ii) As expected, for the interference fit enhancement case alone, the assumption of slip allowed, as compared to no-slip, led to an increase in the cyclic stress concentration from 1.1 to 1.5, while the mean stress was reduced from 604 MPa to 364 MPa.

(iii) The experiments undertaken demonstrated the suitability of the proposed tapered plug/sleeve design to achieve effective interference fitting of an elongated hole. The experimental stress and strain measurements generally agree well with the finite element predictions of (i) above.

(iv) The finite element analysis indicates that the stress distribution due to interference loading is highly non-uniform. Here the hoop stresses are only tensile in the curved ends, and there is a very steep change at the tangent point with the straight sides. This suggests that cold expansion, if required, would only be possible in the curved sections of the hole.

9.2 Elastic-Plastic Analyses

Results obtained from elastic-plastic finite element analyses, assuming no-slip (unless otherwise noted), indicate the following key points:

(i) For the unenhanced open hole, application of the CPLT results in a significant residual tensile hoop stress of 685 MPa, at the critical location on the hole edge. Hence, during application of the sample remote loading, the mean stress was 685 MPa and the cyclic stress concentration was 4.1.

(ii) For both enhancement cases, the stress response was linear during the sample remote loading, with a cyclic stress concentration factor of 1.1.

(iii) Enhancement through combined cold expansion and interference fitting was significantly better that interference fitting alone. For this combined case there was a residual (compressive) hoop stress of -87 MPa, as compared to a residual (tensile) hoop stress of 603 MPa for the interference fitting alone case.

(iv) For the interference fit only enhancement case, the assumption of slip allowed, as compared to no slip, led to a reduction in the mean stress from 603 MPa to 364 MPa, and an increase in the cyclic stress concentration from 1.1 to 1.5. These results are consistent with the fact that when slip is allowed to occur the amount of load transferred between the plug and plate is reduced. Taking into account the comments above in point (ii), it is expected that similar trends will be evident for the case of combined cold expansion and interference fitting.

(v) The stress response for a plate with circular hole as compared to one with an elongated hole is similar for all enhancement cases considered. The only significant difference is that for enhancement through combined cold expansion and interference fitting, the mean stress during subsequent remote loading is significantly lower in magnitude at -87 MPa for the elongated hole case, as compared to -1080 MPa for the circular hole case.

(vi) Overall, enhancement through combined cold expansion with interference fitting is considered highly beneficial, with the favourable stresses generated not being adversely affected by subsequent CPLT.

Acknowledgments

The authors wish to thank Mr P. Piperias for his contributions to the plug design and experimental work presented, and Mr D Rowlands Mr K. Lemm for their technical support. The authors also wish to acknowledge the helpful comments and suggestions given by Mr K. C. Watters, Dr L. F. R. Rose, & Mr J. Paul.

References

1. **KEYS, R.H., MOLENT, L., GRAHAM, A.D.,** *F-111 wing pivot fitting finite element analysis of rework of fuel flow vent hole #13,* DSTO, ARL, Aircraft Structures Technical Memorandum 557, 1992

2. **MANN, J.Y., and JOST, G.S.,** *Stress fields associated with interference fitted and cold-expanded holes, with particular reference to the fatigue life enhancement of aircraft structural joints,* Metals Forum, Vol. 6, No. 1. 1983

3. **ALLAN, R.B. AND HELLER, M.,** *Elastic-plastic stress analysis of a plate containing a round hole with combined cold expansion and interference fitting under F-111C representative loading conditions,* DSTO, AMRL, Technical Report DSTO-TR-0523, File M1/9/167.

4. **BROEK, D.,** *The practical use of fracture mechanics,* Kluwer Academic Publishers, Dordrecht, 1989

5. **JOST, G.S.,** *Stresses and strains in plain and cold worked annuli subjected to remote, interference or combined loading.* DSTO, ARL, Aircraft Structures Report 446, May 1992.

6. **JOST, G.S.,** *Stresses and strains in a cold-worked annulus,* DSTO, ARL, Aircraft Structures Report 434, September 1988.

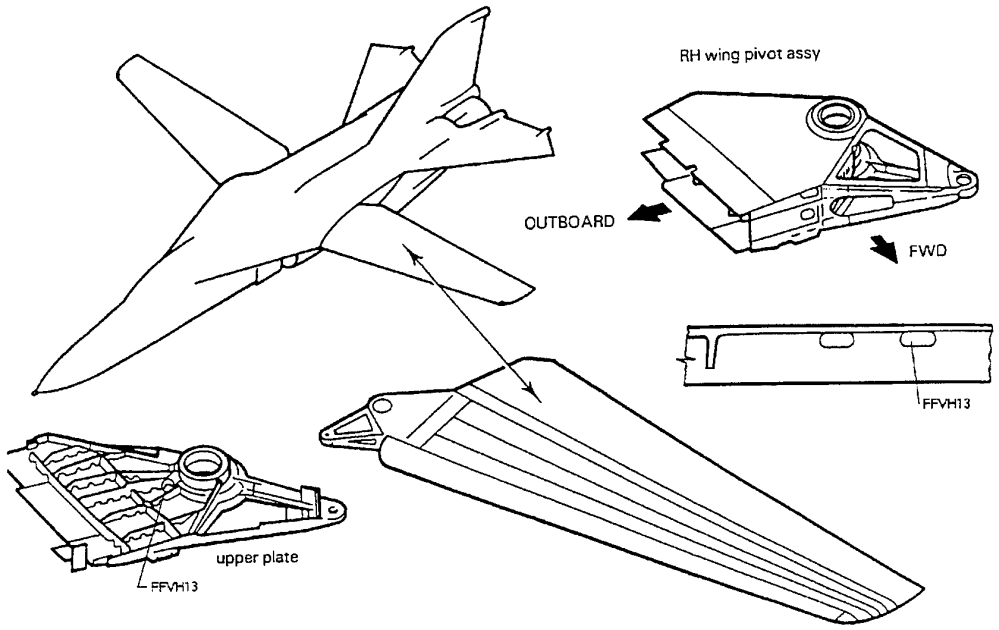

Figure 1. F-111 Aircraft and wing, showing location of fuel flow vent hole number 13 (FFVH13) in the wing pivot fitting.

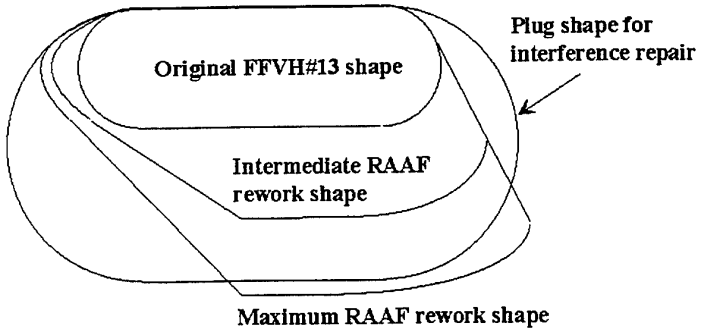

Figure 2. Comparison of original geometry of FFVH13 with typical RAAF rework shapes and proposed hole for interference fit plug.

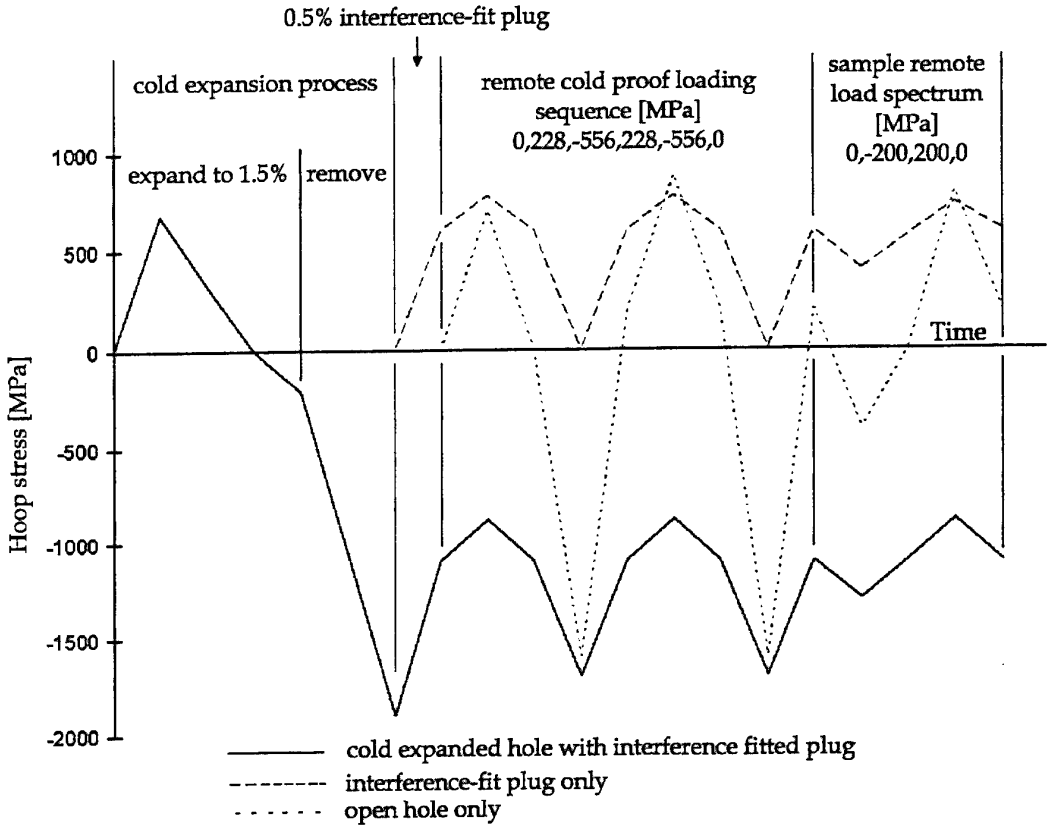

Figure 3. Comparison of finite element hoop stress results at the critical location for rectangular plate containing a circular hole, for various enhancement cases, followed by CPLT and remote spectrum loading.

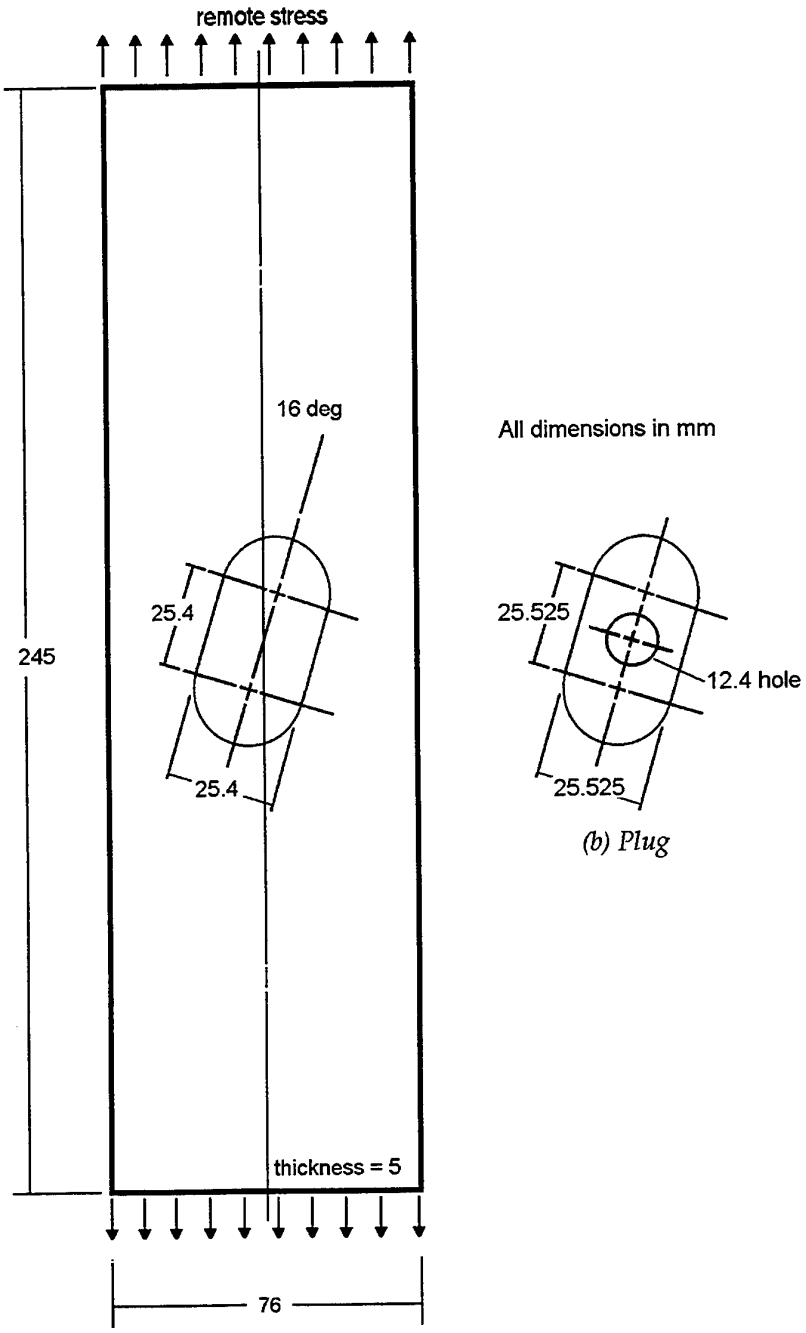

(a) Plate specimen

(b) Plug

Figure 4. Geometry used for two dimensional finite element analysis of an interference fit enhancement of a plate containing an elongated hole, (a) plate, and (b) plug geometry for nominal 0.5 % radial interference level.

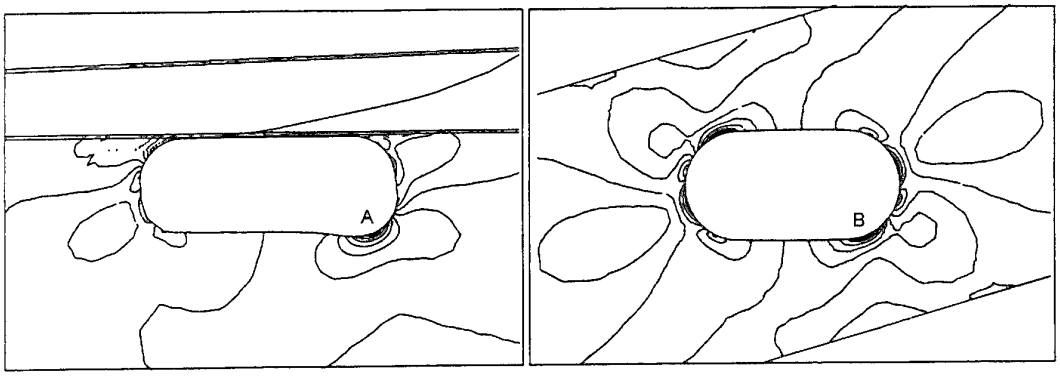

Figure 5. Comparison of elastic finite element results for the von Mises stress distribution in a representative wing substructure model (left), to those obtained from a plate specimen model with a angled hole (right).

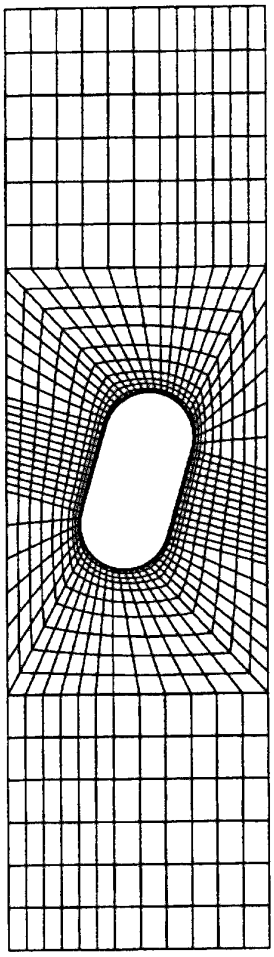

Figure 6. Overall finite element mesh for the plate specimen containing an elongated hole.

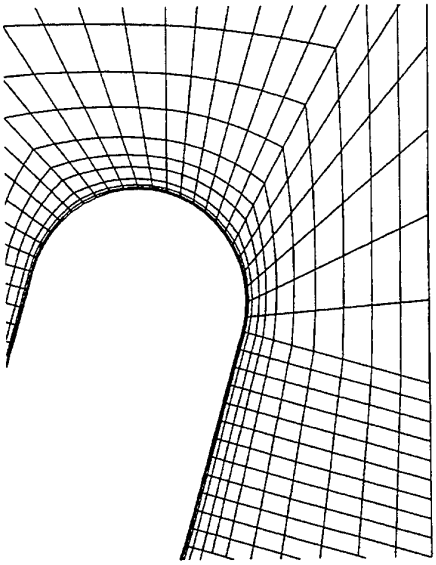

Figure 7. Finite element mesh near the elongated hole for the plate specimen.

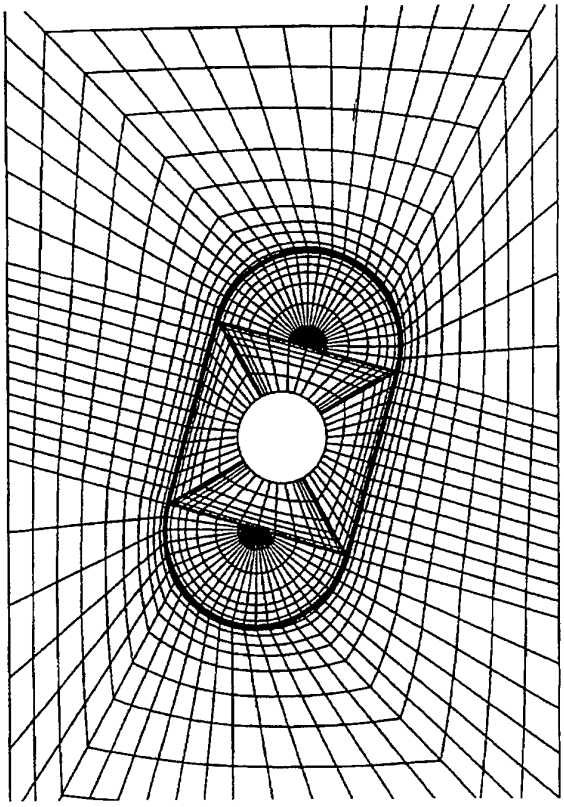

Figure 8. Finite element mesh for specimen with an interference fit plug.

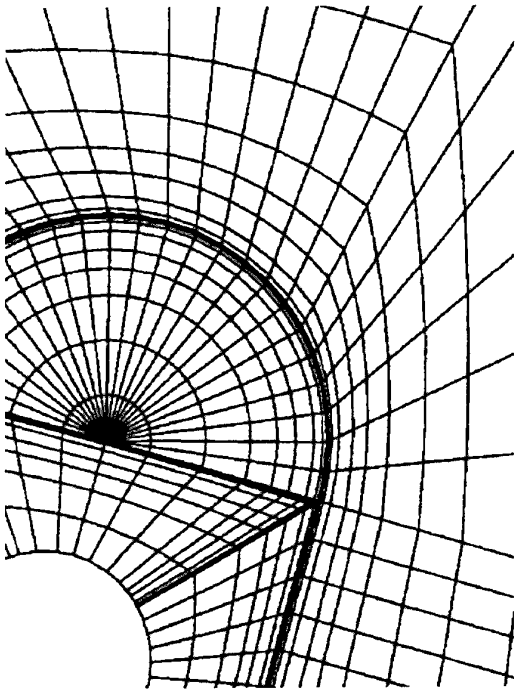

Figure 9. Finite element mesh near the interference fit plug.

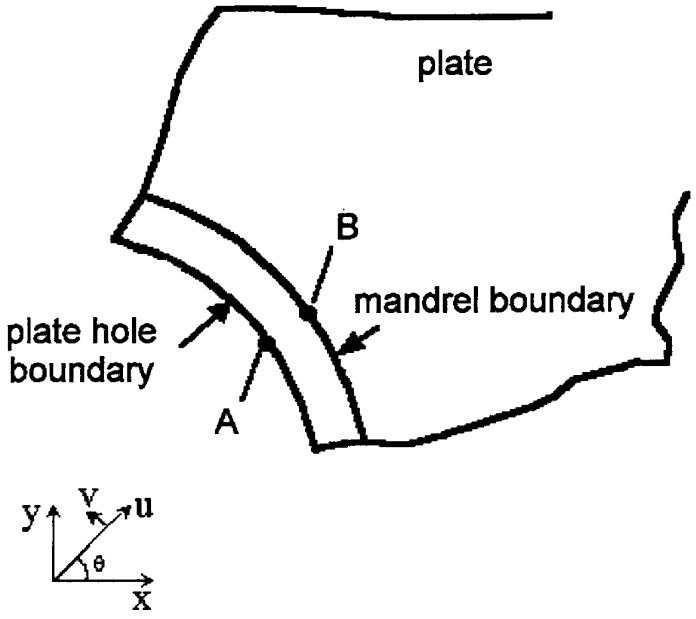

Figure 10. Generic geometry for definition of interference-fit boundary conditions along mandrel/plate interface.

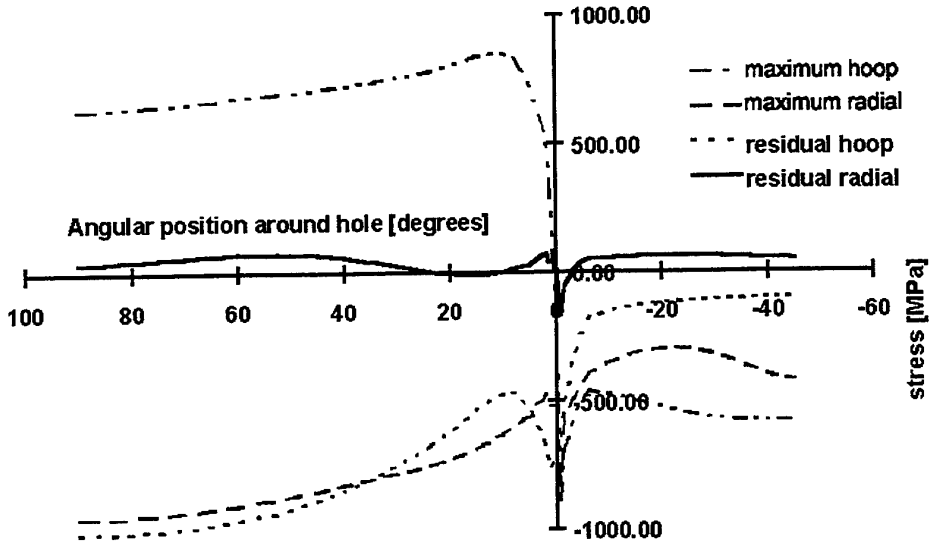

Figure 11. Stress variation around boundary for case given in Section 7 at maximum cold expansion level and at completion of cold expansion.

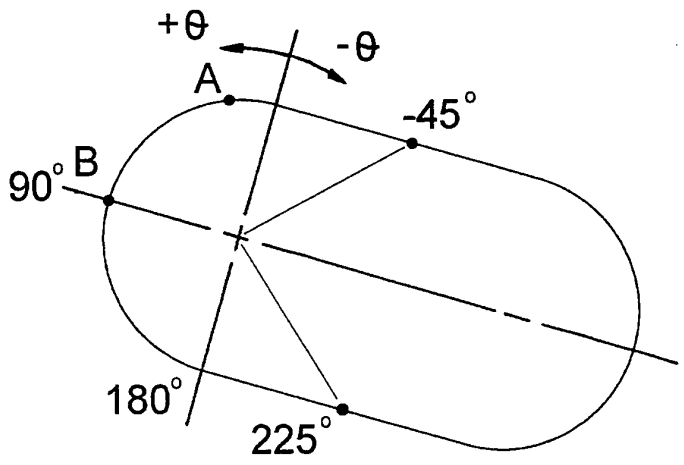

Figure 12. Geometry for definition of angular position around hole boundary, showing critical location at point A.

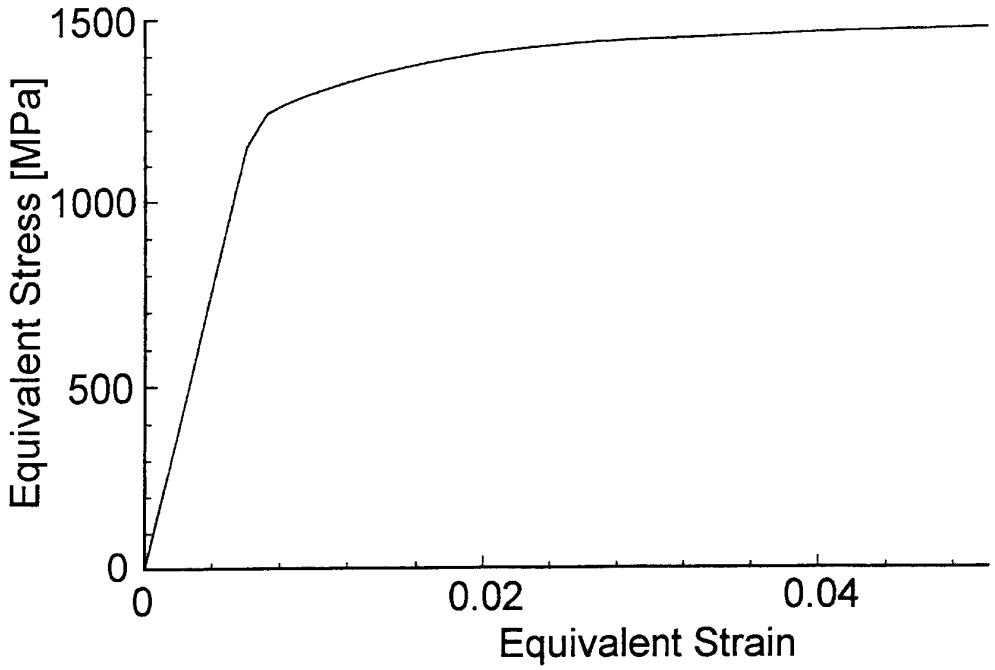

Figure 13. Assumed strain hardening material constitutive response curve for D6ac steel.

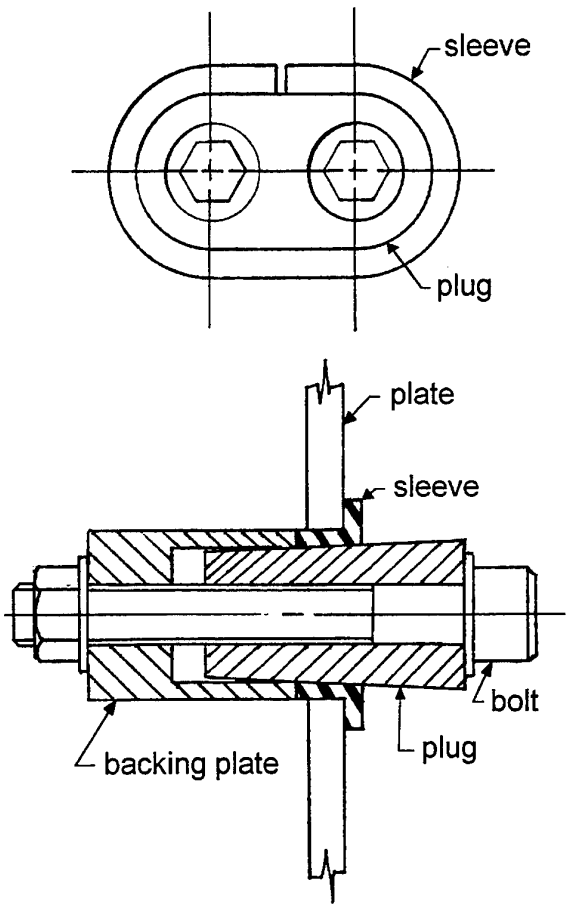

Figure 14. Schematic of interference-fit plug/sleeve design inserted into elongated hole in plate.

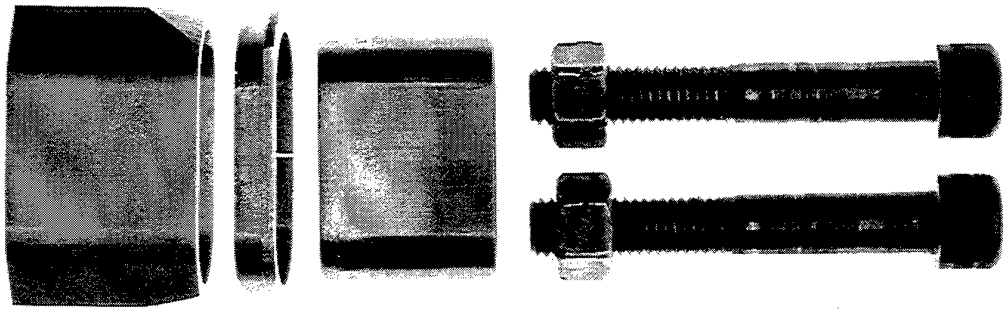

Figure 15. Photograph of key components for interference fit plug design, showing from left to right; backing plate, tapered sleeve, tapered plug and bolts.

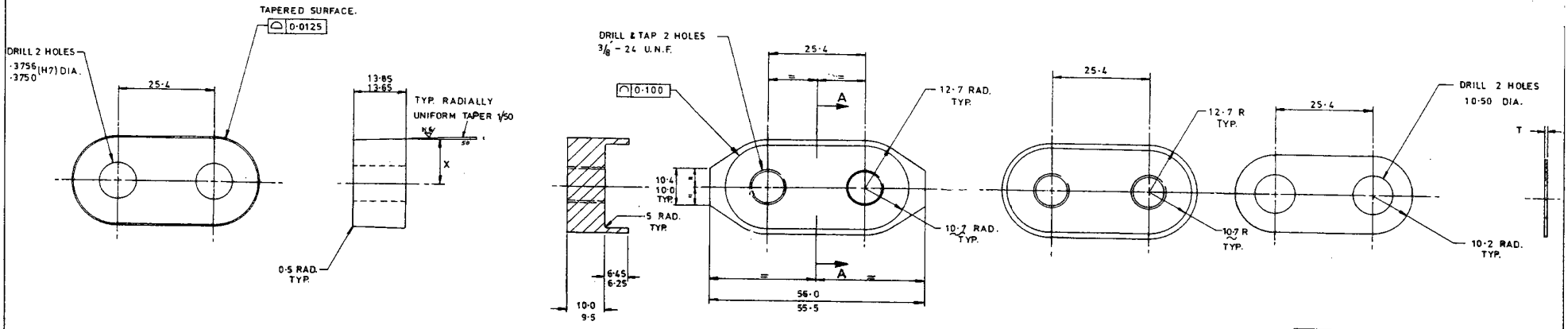

PLUG, TAPER, OVAL.

PART N° SE 5/52/14/RS010-003 (WITH DIMENSION 'X' = 10·794 RAD. TYP.)
PART N° SE 5/52/14/RS010-008 (WITH DIMENSION 'X' = 10·856 RAD. TYP.)
MATERIAL: ALLOY STEEL BAR HEAT TREATED TO
50 ROCKWELL C (U.T.S. 1757 MPa).

BACKING PLATE, TAPER, OVAL.

PART N° SE 5/52/14/RS010-004
MATERIAL: ALLOY STEEL BAR 4340
HEAT TREATED TO
50 ROCKWELL C (U.T.S. 1757 MPa)

BACKING PLATE, TAPER, OVAL.

PART N° SE 5/52/14/RS010 - 009
NOTE: ALL OTHER DIMENSIONS AND
MATERIAL SAME AS
PART N° SE 5/52/14/RS010-004.

PART N°	THICKNESS 'T'
SE 5/52/14/RS 010-005	0·5
SE 5/52/14/RS 010-006	1·0
SE 5/52/14/RS010-007	2·0

SHIM PRELOAD ADJUSTING.

MATERIAL: STAINLESS STEEL COLD DRAWN SHEET TYPE 316.
*

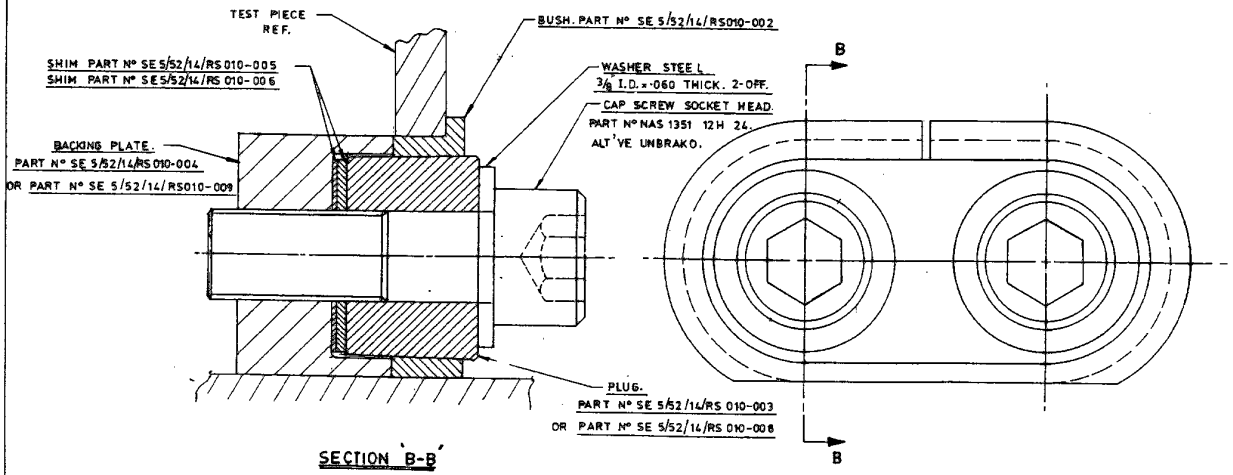

SECTION B-B

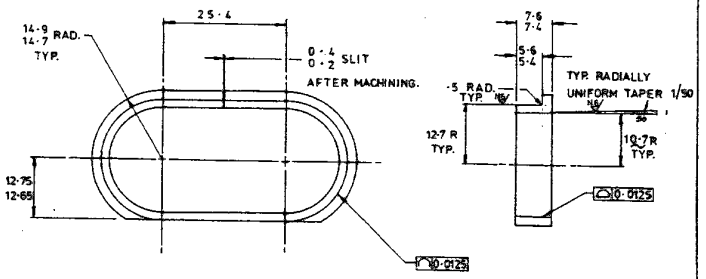

ASSEMBLY PART N° SE 5/52/14/RS010-001

SCALE 4:1

NOTES. 1. BREAK ALL SHARP EDGES AND DEBURR.
*2. MANUFACTURER TO SUPPLY CONFORMANCE
STATEMENT ON MATERIAL USED.
3. SURFACE ROUGHNESS: N8 & NOTED.

BUSH, TAPER, OVAL.

PART N° SE 5/52/14/RS010-002
MATERIAL: STAINLESS STEEL COLD DRAWN BAR TYPE 316.
*

DATE	10-5-84	SCALE: 2:1 & NOTED	DIMENSIONS ARE IN MM.	DRG. PRACTICE - A.S. 1100/1982
DRAWN	P TIKTINAKIS	TOLERANCES: ± 20 mm	DO NOT SCALE	3rd. ANGLE PROJECTION
CHECKED		DSTO - AERONAUTICAL RESEARCH LABORATORY - MELBOURNE, AUSTRALIA		
DESIGN		F 111 TAPER BUSH TEST.		
APPROVED		PLUG, REPAIR, FUEL VENT - (EXPANDING SLEEVE)		DRG. No. SE 5/52/14/RS 010
DIVISION	AED.			REVISION No.
DIV. APP				SHT OF

Figure 16. Engineering drawing of components comprising interference fit assembly.

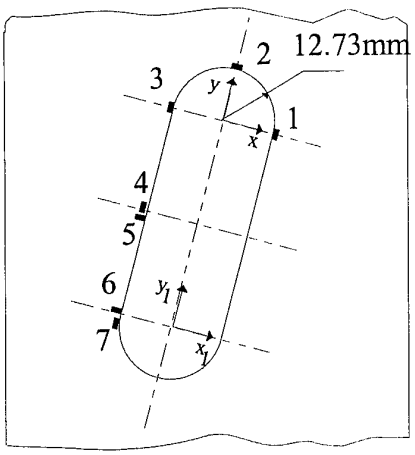

Gauge No.		x (mm)	y (mm)
1	hoop	14.264	-0.105
2	hoop	-0.173	14.507
3	hoop	-14.193	-0.104
		x_1	y_1
4	hoop	-14.666	12.809
5	radial	-15.457	8.52
6	radial	-15.296	1.431
7	hoop	-14.354	-2.683

Figure 17. Orientation and location of strain gauges around hole boundary for plate specimen.

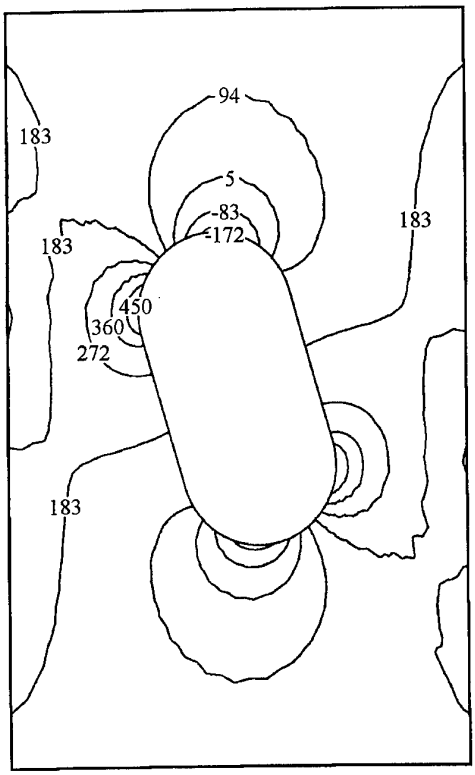

Figure 18. Finite element results for cyclic bulk stress distribution for plate specimen with an unenhanced hole, for a remote loading range of 0 to 100 MPa.

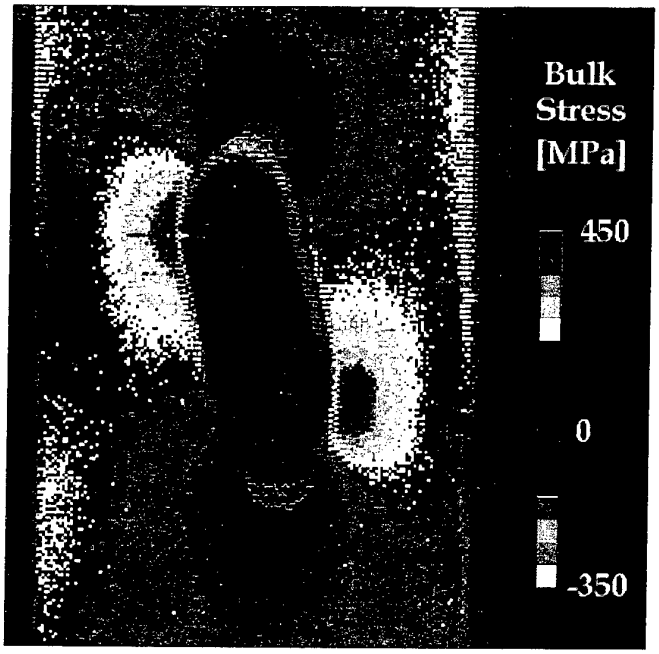

Figure 19. Calibrated SPATE experimental results for cyclic bulk stress distribution for plate specimen with an unenhanced hole, for a remote loading range of 0 to 100 MPa.

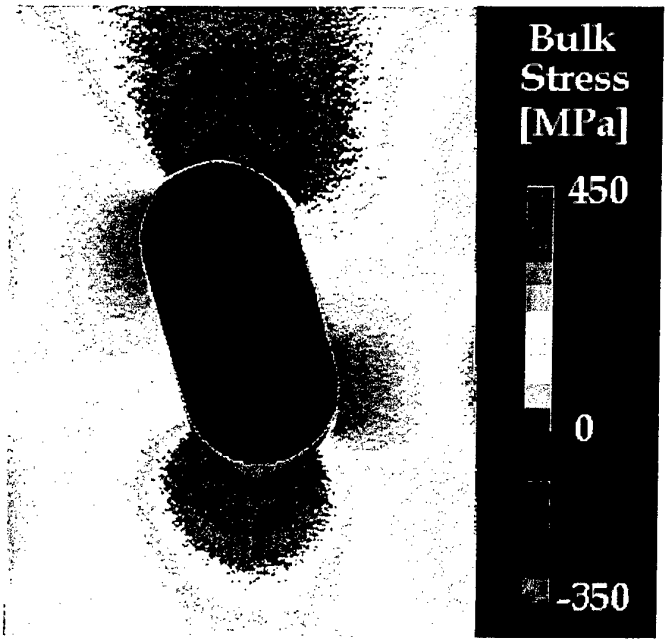

Figure 20. Calibrated FAST experimental results for cyclic bulk stress distribution for plate specimen with an unenhanced hole, for a remote loading range of 0 to 100 MPa.

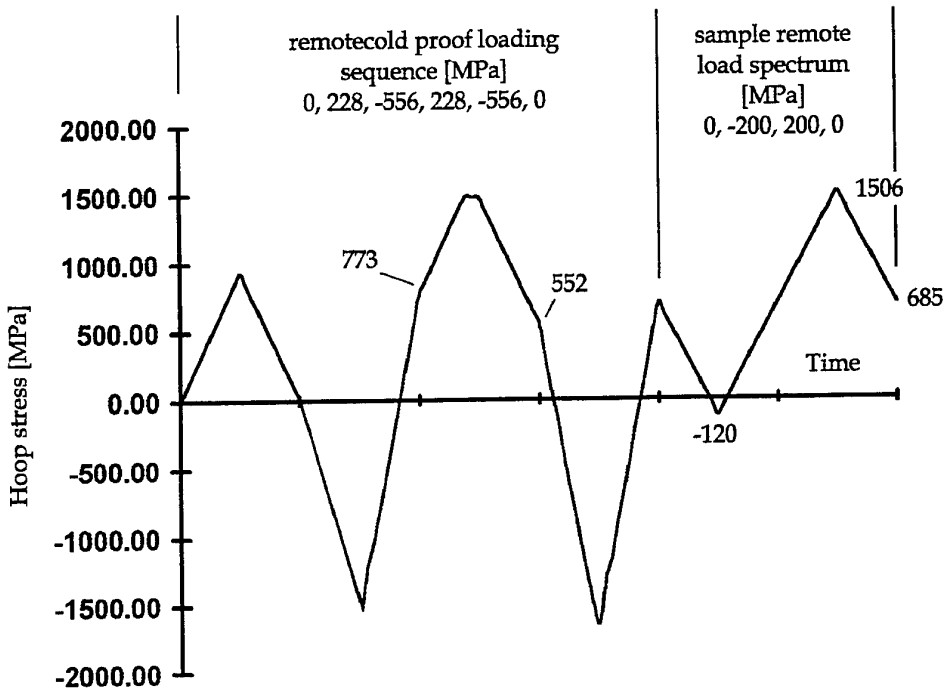

Figure 21. Finite element hoop stress results at the critical location on the hole edge, for the unenhanced plate specimen with CPLT and subsequent remote spectrum loading.

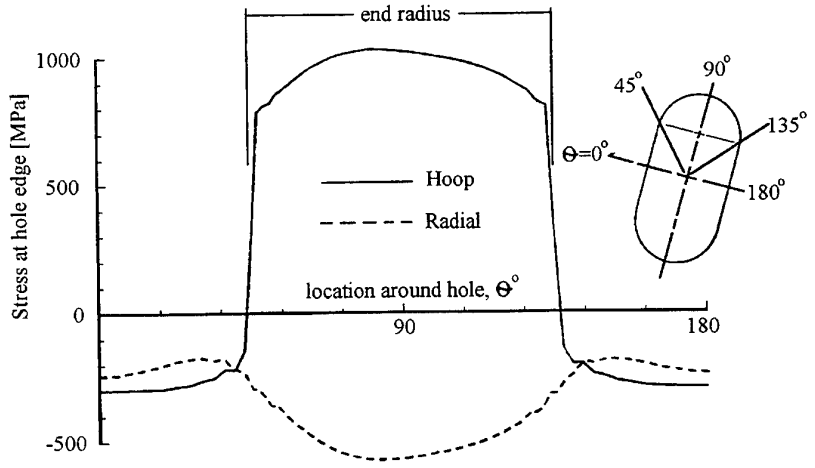

Figure 22. Finite element results for induced stresses in plate specimen around hole boundary, due to a 0.74% interference fit plug.

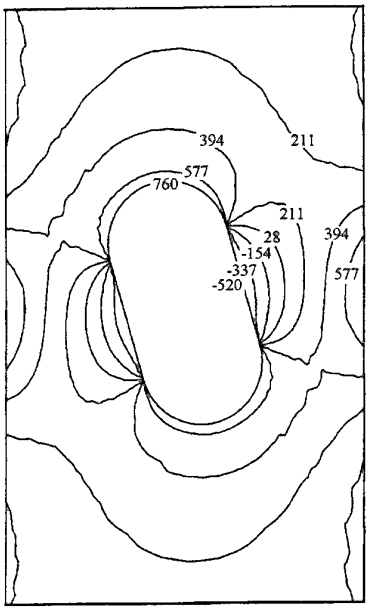

Figure 23. Finite element results for induced bulk stress distribution for plate specimen due to a 0.74% interference fit plug.

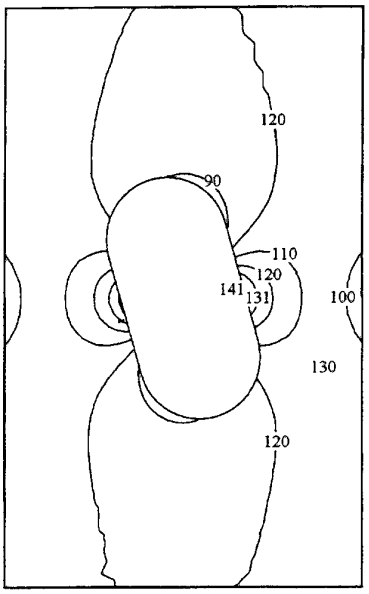

Figure 24. Finite element results for cyclic bulk stress distribution for plate specimen containing an interference fit plug, for a remote loading range of 0 to 100 MPa.

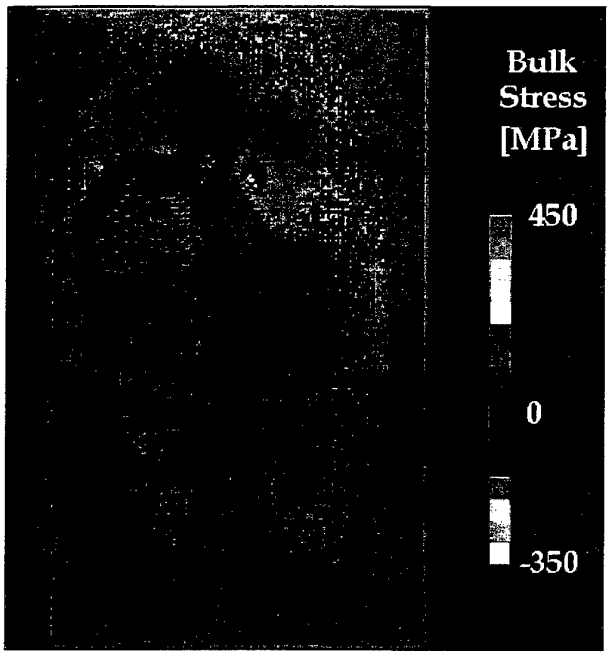

Figure 25. Calibrated SPATE experimental results for cyclic bulk stress distribution for plate specimen with interference fitted plug, for a remote loading range of 0 to 100 MPa.

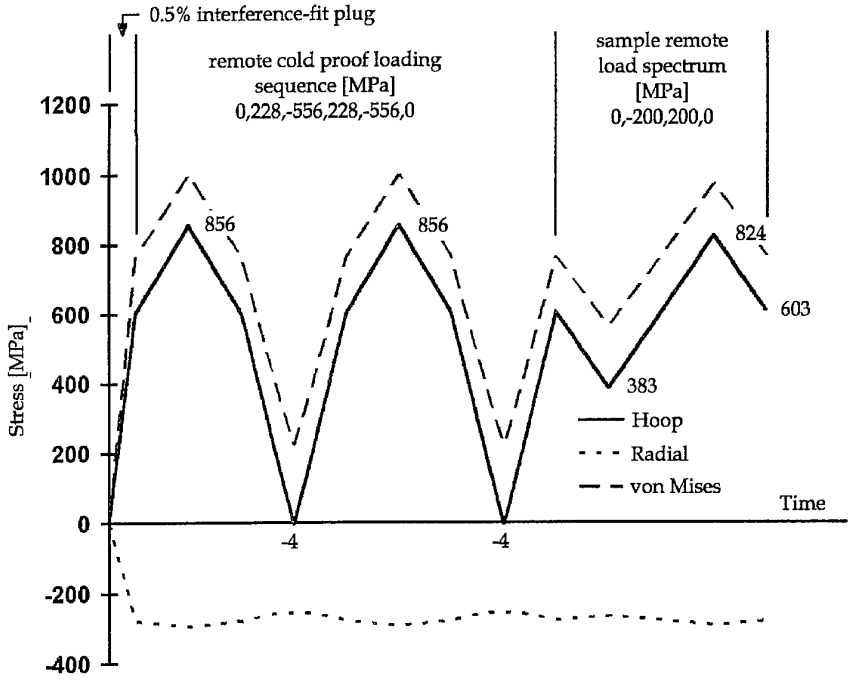

Figure 26. Finite element stress results at critical location for plate specimen containing an interference fit plug, with subsequent CPLT and sample remote loading, assuming no slip.

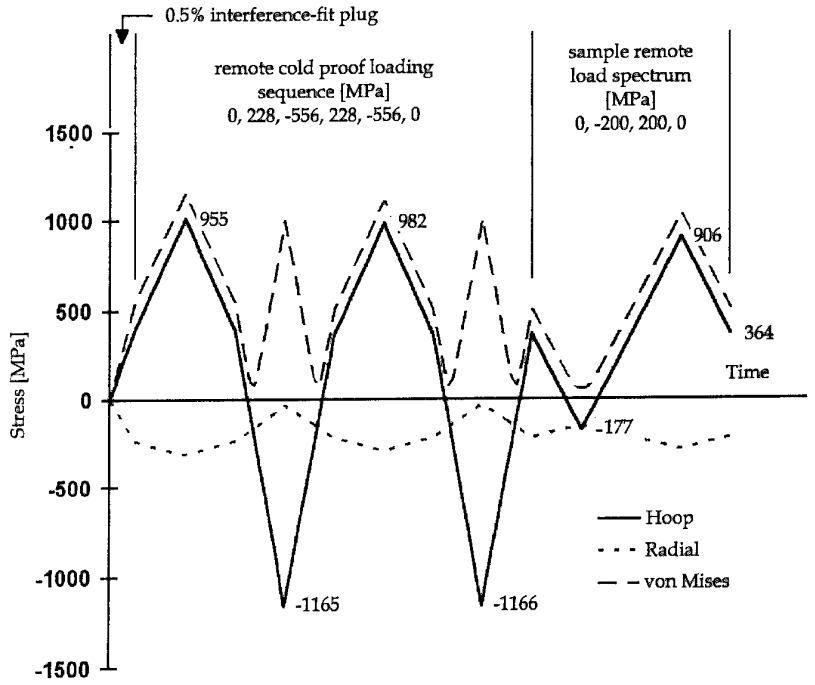

Figure 27. Finite element stress results at critical location for plate specimen containing an interference fit plug, with subsequent CPLT and sample remote loading, with slip allowed.

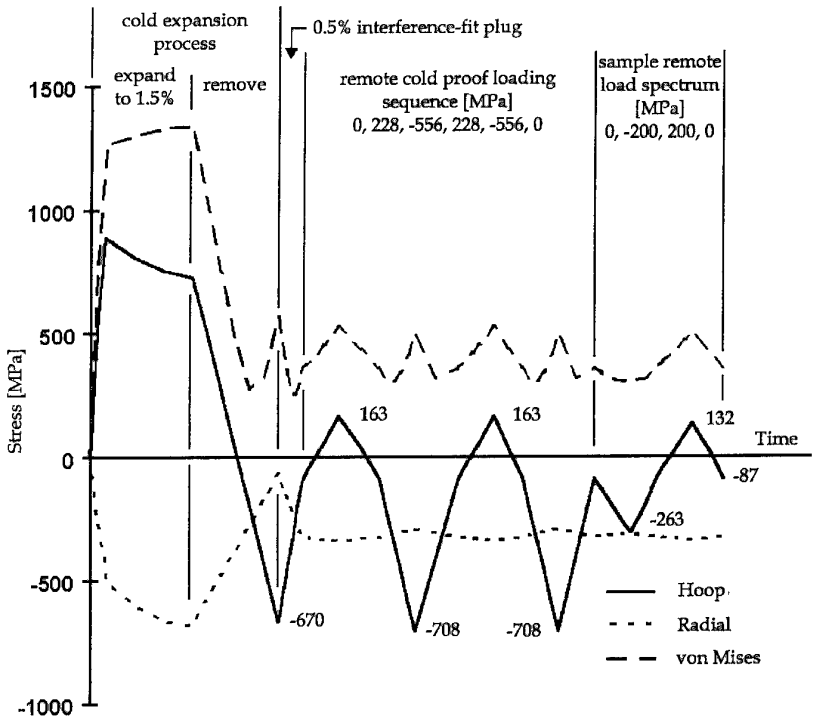

Figure 28. Finite element stress results at critical location for plate specimen with a cold expanded hole containing an interference fitted plug, with subsequent CPLT and sample remote loading.

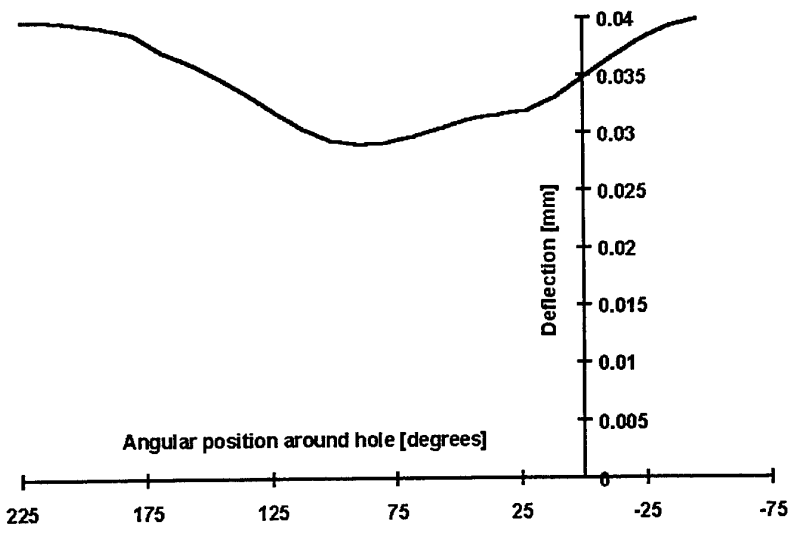

Figure 29. Variation of residual hole boundary deflection in plate specimen due to 1.5% cold expansion process, with angular position as defined in Figure 12.

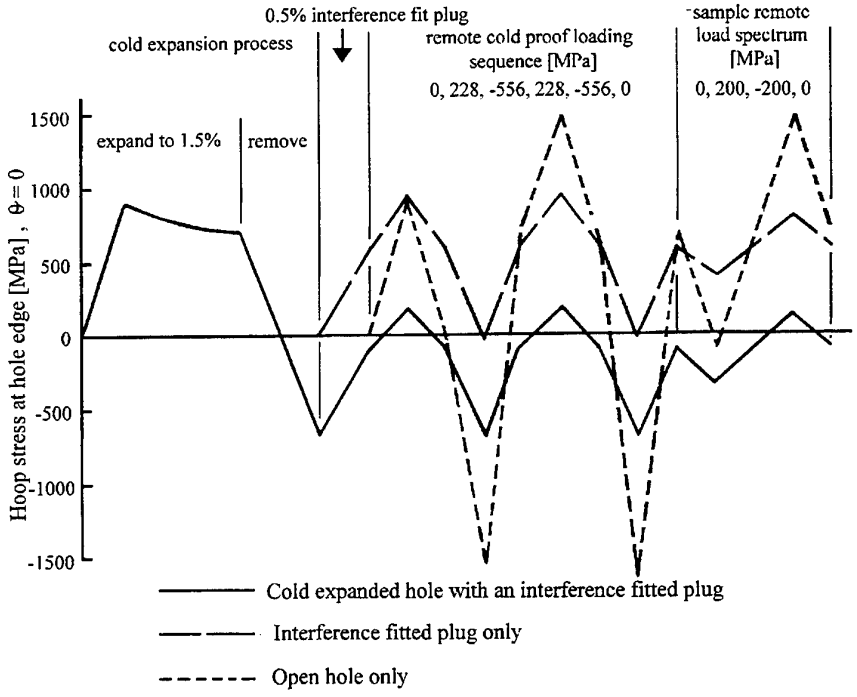

Figure 30. Comparison of finite element hoop stress results at critical location for plate specimen with an elongated hole, for various enhancement cases, followed by CPLT and remote spectrum loading.

DISTRIBUTION LIST

Stress Analysis of an Interference Fit Life Extension Option for a Cold Expanded Elongated Fuel flow vent Hole on the F-111C Aircraft

R. B. Allan and M. Heller

AUSTRALIA

1. DEFENCE ORGANISATION

a. Task Sponsor AIR OIC ASI-LSA

b. S&T Program

Chief Defence Scientist
FAS Science Policy
AS Science Corporate Management
} shared copy

Director General Science Policy Development
Counsellor Defence Science, London (Doc Data Sheet)
Counsellor Defence Science, Washington (Doc Data Sheet)
Scientific Adviser to MRDC Thailand (Doc Data Sheet)
Director General Scientific Advisers and Trials/Scientific Adviser Policy and Command (shared copy)
Navy Scientific Adviser (Doc Data Sheet and distribution list only)
Scientific Adviser - Army (Doc Data Sheet and distribution list only)
Air Force Scientific Adviser
Director Trials

Aeronautical and Maritime Research Laboratory
Director

Chief of Airframe and Engines Division
Research Leader Fracture Mechanics
Research Leader Structural Integrity
Research Leader Aerospace Composites
K. Watters
G. Clark
D. Graham
I. Anderson
L. Molent
D. Lombardo
P. Piperias
R.B. Allan (5 copies)
M. Heller (5 copies)

DSTO Library
Library Fishermens Bend
Library Maribyrnong
Library Salisbury (2 copies)
Australian Archives
Library, MOD, Pyrmont (Doc Data sheet only)

c. **Capability Development Division**
Director General Maritime Development (Doc Data Sheet only)
Director General Land Development (Doc Data Sheet only)
Director General C3I Development (Doc Data Sheet only)

d. **Navy**
SO (Science), Director of Naval Warfare, Maritime Headquarters Annex, Garden Island, NSW 2000. (Doc Data Sheet only of Navy and FD (Sea) sponsored reports)

e. **Army**
ABCA Office, G-1-34, Russell Offices, Canberra (4 copies)

f. **Air Force**
CENG 501 WING, AMBERLY
OIC ATF ATS, RAAFSTT, WAGGA (2 copies)

g. **Intelligence Program**
Defence Intelligence Organisation
Library, Defence Signals Directorate (Doc Data Sheet only)

i. **Corporate Support Program (libraries)**
OIC TRS, Defence Regional Library, Canberra
Officer in Charge, Document Exchange Centre (DEC), 1 copy
*US Defence Technical Information Centre, 2 copies
*UK Defence Research Information Center, 2 copies
*Canada Defence Scientific Information Service, 1 copy
*NZ Defence Information Centre, 1 copy
National Library of Australia, 1 copy

2. **UNIVERSITIES AND COLLEGES**

Australian Defence Force Academy
Library
Head of Aerospace and Mechanical Engineering
Deakin University, Serials Section (M list), Deakin University Library, Geelong, 3217
Senior Librarian, Hargrave Library, Monash University
Librarian, Flinders University

3. **OTHER ORGANISATIONS**

NASA (Canberra)
AGPS

OUTSIDE AUSTRALIA

4. **ABSTRACTING AND INFORMATION ORGANISATIONS**
INSPEC: Acquisitions Section Institution of Electrical Engineers
Library, Chemical Abstracts Reference Service
Engineering Societies Library, US

Materials Information, Cambridge Scientific Abstracts, US
Documents Librarian, The Center for Research Libraries, US

5. **INFORMATION EXCHANGE AGREEMENT PARTNERS**
Acquisitions Unit, Science Reference and Information Service, UK
Library - Exchange Desk, National Institute of Standards and Technology, US
National Aerospace Laboratory, Japan
National Aerospace Laboratory, Netherlands

SPARES (10 copies)

Total number of copies: 76

DEFENCE SCIENCE AND TECHNOLOGY ORGANISATION
DOCUMENT CONTROL DATA

1. PRIVACY MARKING/CAVEAT (OF DOCUMENT)

2. TITLE

Stress Analysis of an Interference Fit Life Extension Option for a Cold Expanded Elongated Fuel Flow Vent Hole on the F-111C Aircraft

3. SECURITY CLASSIFICATION (FOR UNCLASSIFIED REPORTS THAT ARE LIMITED RELEASE USE (L) NEXT TO DOCUMENT CLASSIFICATION)

Document (U)
Title (U)
Abstract (U)

4. AUTHOR(S)

R. B. Allan & M. Heller

5. CORPORATE AUTHOR

Aeronautical and Maritime Research Laboratory
PO Box 4331
Melbourne Vic 3001

6a. DSTO NUMBER	6b. AR NUMBER	6c. TYPE OF REPORT	7. DOCUMENT DATE
DSTO-TR-0549	AR-010-256	Technical Report	June 1997

8. FILE NUMBER	9. TASK NUMBER	10. TASK SPONSOR	11. NO. OF PAGES	12. NO. OF REFERENCES
M1/9/107	95/228	AIR OIC ASI-LSA	33	6

13. DOWNGRADING/DELIMITING INSTRUCTIONS

None

14. RELEASE AUTHORITY

Chief, Airframes and Engines Division

15. SECONDARY RELEASE STATEMENT OF THIS DOCUMENT

Approved for public release

OVERSEAS ENQUIRIES OUTSIDE STATED LIMITATIONS SHOULD BE REFERRED THROUGH DOCUMENT EXCHANGE CENTRE, DIS NETWORK OFFICE, DEPT OF DEFENCE, CAMPBELL PARK OFFICES, CANBERRA ACT 2600

16. DELIBERATE ANNOUNCEMENT

No Limitations

17. CASUAL ANNOUNCEMENT Yes

18. DEFTEST DESCRIPTORS

fatigue life, finite element analysis, F-111C wing pivot fittings, stress analysis, holes (openings), cold working, expansion

19. ABSTRACT

This investigation has been undertaken as part of a program of work having the aim of determining a suitable fatigue life enhancement option for the non-circular fuel flow vent hole number 13 in the wing pivot fitting of the F-111C aircraft. Two types of stress analysis have been undertaken for a finite width rectangular plate of D6ac steel containing an elongated hole. Firstly, plate stress distributions due to interference fitting obtained from elastic two dimensional finite element analyses were compared to those measured experimentally using strain gauges and thermoelasticity. Secondly, two-dimensional elastic-plastic finite element analyses were undertaken to quantify the effect on critical plate stresses due to enhancement by combined cold expansion with interference fitting, in the presence of subsequent representative cold proof test loading and a sample spectrum loading. The predicted stresses for the elastic analysis cases agreed well with the experimental results, which also demonstrated the suitability of a proposed tapered plug/sleeve design to achieve effective interference fitting of an elongated hole. Overall, enhancement through combined cold expansion and interference fitting was considered to be significantly better than interference fitting alone. For example, the combined enhancement case, as compared to interference fitting only, led to a change in the critical hoop stress from 603 MPa, to -87 MPa. These favourable results indicate that such an enhancement procedure would potentially be suitable for extending the fatigue life of the fuel flow vent hole number 13 region of the F-111C aircraft, pending the results of appropriate static and fatigue tests.